JOC Article

A Combined NMR, DFT, and X-ray Investigation of Some Cinchona Alkaloid *O*-Ethers

Igor Busygin,[†] Ville Nieminen,[‡] Antti Taskinen,[‡] Jari Sinkkonen,[§] Esa Toukoniitty,[‡] Reijo Sillanpää,[⊥] Dmitry Yu. Murzin,[‡,*] and Reko Leino[†,*]

Laboratories of Organic Chemistry and Industrial Chemistry and Reaction Engineering, Åbo Akademi University, FI-20500 Turku, Finland, Department of Chemistry, University of Turku, FI-20014 Turku, Finland, and Department of Chemistry, University of Jyväskylä, FI-40351 Jyväskylä, Finland

dmitry.murzin@abo.fi; reko.leino@abo.fi

Received April 18, 2008

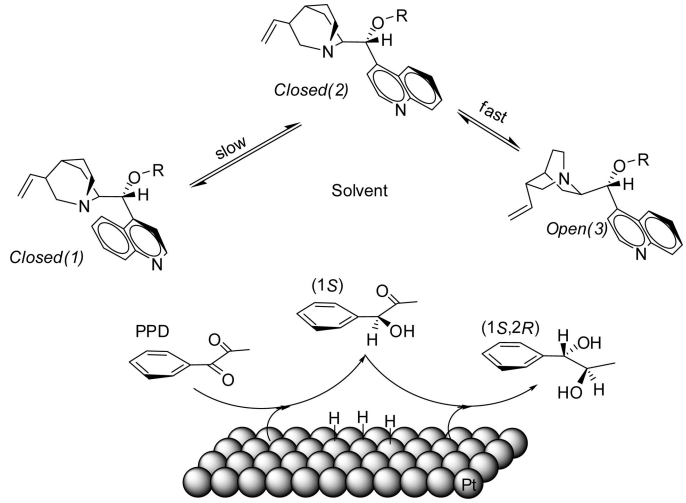

Structures and conformational behavior of several cinchona alkaloid *O*-ethers in the solid state (X-ray), in solution (NMR and DFT), and in the gas phase (DFT) were investigated. In the crystal, *O*-phenylcinchonidine adopts the Open(3) conformation similar to cinchonidine, whereas the *O*-methyl ether derivatives of both cinchonidine and cinchonine are packed in the *Closed(1)* conformation. Dynamic equilibria in solutions of the alkaloids were revealed by combined experimental-theoretical spin simulation/iteration techniques for the first time. In the ^{1}H NMR spectra in $CDCl_3$ and toluene-d_8 at room temperature, *Closed(1)* conformation was observed for the *O*-silyl ethers as a separate set of signals. For *O*-methyl ether derivatives *Closed(1)* could be separated only at −30 °C in $CDCl_3$ or toluene-d_8 and for *O*-phenylcinchonidine at −70 °C in $CDCl_3/CD_2Cl_2$. The ratio between the *Closed(2)* and *Open(3)* conformers was estimated by analyzing the vicinal coupling constant $^3J_{H9,H8}$ at ambient and low temperatures. The observed conformational equilibria of *O*-(*tert*-butyldimethylsilyl)cinchonidine in $CDCl_3$ and toluene-d_8 are in good agreement with the theoretically estimated equilibrium populations of the conformations according to Boltzmann statistics. The conformational equilibria of four cinchona alkaloid *O*-ether solutes in $CDCl_3$ and toluene-d_8 are discussed in the light of their relevance to the mechanism of 1-phenyl-1,2-propanedione (PPD) hydrogenation over cinchona alkaloid modified heterogeneous platinum catalysts. It was demonstrated that the conformation found to be abundant in the liquid phase has no direct correlation with the enantioselectivity of the PPD hydrogenation reaction.

1. Introduction

Cinchona alkaloids are an important class of natural chiral compounds that have found wide use, e.g., as pharmaceuticals and chiral resolving agents for separation of optical isomers and in catalytic applications as catalysts and as chiral auxiliaries. To the most studied applications of cinchona alkaloids belong their use as chiral modifiers in heterogeneous catalysis[1] and as organocatalysts for asymmetric homogeneous transformations.[2]

[†] Laboratory of Organic Chemistry, Åbo Akademi University.
[‡] Laboratory of Industrial Chemistry and Reaction Engineering, Åbo Akademi University.
[§] University of Turku.
[⊥] University of Jyväskylä.

(1) (a) Mallat, T.; Orglmeister, E.; Baiker, A. *Chem. Rev.* **2007**, *107*, 4863–4890. (b) Bartók, M. *Curr. Org. Chem.* **2006**, *10*, 1533–1567. (c) Murzin, D. Yu.; Mäki-Arvela, P.; Toukoniitty, E.; Salmi, T. *Catal. Rev.* **2005**, *47*, 175–256. (d) Hutchings, G. J. *Annu. Rev. Mater. Res.* **2005**, *35*, 143–166. (e) Studer, M.; Blaser, H.-U; Exner, C. *Adv. Synth. Catal.* **2003**, *345*, 45–65. (f) Baddeley, C. J. *Top. Catal.* **2003**, *25*, 17–28.

10.1021/jo8008462 CCC: $40.75 © 2008 American Chemical Society
Published on Web 08/07/2008

SCHEME 1. Enantioselective Hydrogenation of 1 over Pt/Al_2O_3 Modified by Cinchona Alkaloid Derivatives

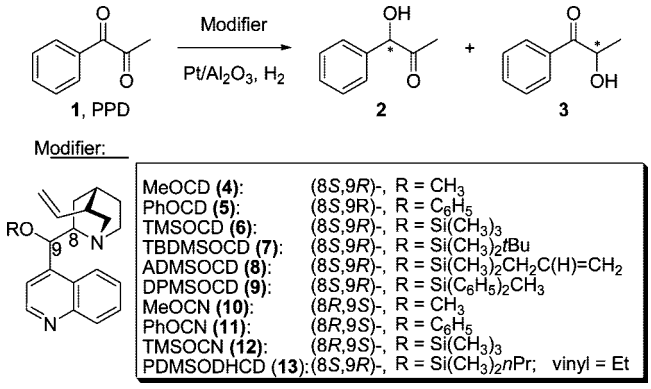

Numerous derivatives of naturally occurring (−)-cinchonidine (CD) and (+)-cinchonine (CN) have been synthesized and utilized in both heterogeneous[1,3] and homogeneous[2,4] enantioselective reactions in order to approach the mechanism of chiral induction.

Recently, *O*-ether derivatives of cinchona alkaloids have attracted considerable attention, as in several hydrogenation reactions over chirally modified surfaces, they are capable of inverting the sense of enantioselectivity when compared to the reaction over the parent alkaloid modified surface.[5] In the present study, we have investigated the substituent effect on the conformational equilibria of some cinchona alkaloid *O*-ethers as well as on their structural behavior upon crystallization. In an earlier related investigation, we employed nine derivatives of cinchonidine and cinchonine possessing substituents with different nature and bulkiness as chiral modifiers in the enantioselective hydrogenation of 1-phenyl-1,2-propanedione (PPD, **1**) (Scheme 1).[5e] Here, we present the synthesis of these modifiers, together with their detailed structural characterization and conformational studies by X-ray crystallographic structure determinations, by NMR spectroscopic analysis, and by DFT calculations.

Assessing the dynamics of cinchona alkaloids is important in developing a comprehensive understanding of the mechanisms of enantiodifferentiation in catalytic reactions. Cinchona alkaloids consist of two rigid moieties, a quinoline ring and a quinuclidine ring, coupled together by two carbon−carbon bonds (Scheme 1). The relative position of these two parts determines the conformational diversity of the alkaloid. Several open and closed conformations are known for cinchonidine,[6] as studied by both NMR[6a–c] and molecular modeling.[6a,d,e] It is well-known that in apolar solvents cinchonidine preferentially adopts the so-called *Open(3)* conformation with the population of approximately 60−70%.[6a] A substituent at the C(9)-*O*- position, however, hinders the rotation around the C4′-C9 and C9−C8 bonds (for atom numbering see Supporting Information) and alters the conformational equilibria.[6b] The modified conformations are illustrated in Figure 1 as Newman projections.

In most mechanistic proposals for chirally modified hydrogenation catalysts, cinchonidine is assumed to interact with the carbonyl substrate in *Open(3)* conformation,[7a–f] its most abundant conformer in liquid-phase.[6] A correlation between the population of *Open(3)* conformation in different solvents and the experimental enantiomeric excess (ee) observed in the hydrogenation of ketopantolactone has been reported.[6a] Modifier rigidity has also been taken as a proof of the crucial role of the *Open(3)* conformation.[8] The phenomenon of switching the enantiodifferentiating properties of the catalyst by changing the modifier structure has stimulated an interest for studying the conformational properties of cinchona alkaloid *O*-ethers. Baiker and co-workers have studied the adsorption of *O*-phenylcinchonidine (PhOCD),[9a,b] *O*-(trimethylsilyl)cinchonidine,[9c] and *O*-methylcinchonidine[9c] on platinum by DFT and ATR-IR, as well as the conformational equilibria of PhOCD in different solvents by vibrational circular dichroism (VCD) spectroscopy.[9c]

Despite significant progress in the experimental techniques and theoretical methods, the mechanism of enantiodifferentiation in the hydrogenation of activated ketones over cinchona alkaloid modified metal catalysts remains unclear in many respects.[1] Several models have been proposed in order to describe the origin of enantioselectivity over chirally modified metal catalysts.[7] The majority of the earlier mechanistic models have utilized the chiral modifier with its quinoline aromatic system adsorbed parallel to the metal surface. It is commonly assumed, although not experimentally confirmed, that the π-bonded modifier species interacts with the substrate on the metal surface, thus steering the production of one enantiomer in excess over the other.[1,10] Recently, tilting of the quinoline ring relative to the metal surface was reported for the adsorption of cinchona alkaloids at saturation coverage.[11] A potential involvement of

(2) (a) France, S.; Guerin, D. J.; Miller, S. J.; Letcka, T. *Chem. Rev.* **2003**, *103*, 2985–3012. (b) Tian, S.-K.; Chen, Y.; Hang, J.; Tang, L.; McDaid, P.; Deng, L. *Acc. Chem. Res.* **2004**, *37*, 621–631. Kacprzak, K.; Gawroński, J. *Synthesis* **2001**, 961–998. (d) *Enantioselective Organocatalysis: Reactions and Experimental Procedures*; Dalko, P. I., Ed.; Wiley-VCH: Weinheim, 2007. (e) *New Frontiers in Asymmetric Catalysis*; Mikami, K., Lautens, M., Eds.; Wiley-VCH: Weinheim, 2007. (f) Berkessel, A.; Gröger, H. *Asymmetric Organocatalysis*; Wiley-VCH: Weinheim, 2005.

(3) (a) Blaser, H. U.; Jalett, H. P.; Lottenbach, W.; Studer, M. *J. Am. Chem. Soc.* **2000**, *122*, 12675–12682. (b) Exner, C.; Pfaltz, A.; Studer, M.; Blaser, H.-U. *Adv. Synth. Catal.* **2003**, *345*, 1253–1260. (c) Busygin, I.; Toukoniitty, E.; Sillanpää, R.; Murzin, D. Yu.; Leino, R. *Eur. J. Org. Chem.* **2005**, 2811–2821. (d) Busygin, I.; Toukoniitty, E.; Murzin, D. Yu.; Leino, R. *J. Mol. Catal. A: Chem.* **2005**, *236*, 227–235.

(4) (a) Seitz, T.; Baudoux, J.; Bekolo, H.; Cahard, D.; Plaquevent, J.-C.; Lasne, M.-C.; Rouden, J. *Tetrahedron* **2006**, *62*, 6155–6165. (b) Merschaert, A.; Delbeke, P.; Daloze, D.; Dive, G. *Tetrahedron Lett.* **2004**, *45*, 4697–4701.

(5) (a) Diezi, S.; Szabo, A.; Mallat, T.; Baiker, A. *Tetrahedron: Asymmetry* **2003**, *14*, 2573–2577. (b) Sonderegger, O. J.; Ho, G. M. W.; Bürgi, T.; Baiker, A. *J. Mol. Catal. A: Chem.* **2005**, *229*, 19–24. (c) Cserényi, S.; Felföldi, K.; Balázsik, K.; Szöllősi, G.; Bucsi, I.; Bartók, M. *J. Mol. Catal. A: Chem.* **2006**, *247*, 108–115. (d) Toukoniitty, E.; Busygin, I.; Leino, R.; Murzin, D. Yu. *J. Catal.* **2004**, *227*, 210–216. (e) Busygin, I.; Wärnå, J.; Toukoniitty, E.; Murzin, D. Yu.; Leino, R. *J. Catal.* **2008**, *254*, 339–348.

(6) (a) Bürgi, T.; Baiker, A. *J. Am. Chem. Soc.* **1998**, *120*, 12920–12926. (b) Dijkstra, G. D. H.; Kellogg, R. M.; Wynberg, H.; Svendsen, J. S.; Marko, I.; Sharpless, K. B. *J. Am. Chem. Soc.* **1989**, *111*, 8069–8076. (c) Dijkstra, G. D. H.; Kellogg, R. M.; Wynberg, H. *J. Org. Chem.* **1990**, *55*, 6121–6231. (d) Lindholm, A.; Mäki-Arvela, P.; Toukoniitty, E.; Pakkanen, T. A.; Hirvi, J. T.; Salmi, T.; Murzin, D. Yu.; Sjöholm, R.; Leino, R. *J. Chem. Soc. Perkin Trans. 1* **2002**, 2605–2612. (e) Schürch, M.; Schwalm, O.; Mallat, T.; Weber, J.; Baiker, A. *J. Catal.* **1997**, *169*, 275–286. (f) Martinek, T. A.; Varga, T.; Fülöp, F.; Bartók, M. *J. Catal.* **2007**, *246*, 266–276.

(7) (a) Sutherland, I. M.; Ibbotson, A.; Moyes, R. B.; Wells, P. B. *J. Catal.* **1990**, *125*, 77–88. (b) Augustine, R. L.; Taneilyan, S. K.; Doyle, L. K. *Tetrahedron: Asymmetry* **1993**, *4*, 1803–1827. (c) Vayner, G.; Houk, K. N.; Sun, Y.-K. *J. Am. Chem. Soc.* **2004**, *126*, 199–203. (d) Schwalm, O.; Minder, B.; Weber, J.; Baiker, A. *Catal. Lett.* **1994**, *23*, 271–279. (e) Baiker, A. *J. Mol. Catal. A: Chem.* **2000**, *163*, 205–220. (f) Lavoie, S.; Laliberté, M.-A.; McBreen, P. H. *J. Am. Chem. Soc.* **2006**, *128*, 7588–7593. (g) Margitfalvi, J. L.; Hegedüs, M. *J. Mol. Catal. A: Chem.* **1996**, *107*, 281–289.

(8) (a) Bartók, M.; Sutyinszki, M.; Felföldi, K.; Szöllösi, G. *Chem. Commun.* **2002**, 1130–1131. (b) Margitfalvi, J. L.; Tálas, E. *Appl. Catal., A* **2006**, *301*, 187–195.

(9) (a) Bonalumi, N.; Vargas, A.; Ferri, D.; Bürgi, T.; Mallat, T.; Baiker, A. *J. Am. Chem. Soc.* **2005**, *127*, 8467–8477. (b) Vargas, A.; Ferri, D.; Bonalumi, N.; Mallat, T.; Baiker, A. *Angew. Chem., Int. Ed.* **2007**, *46*, 3905–3908. (c) Bonalumi, N.; Vargas, A.; Ferri, D.; Baiker, A. *Chem. Eur. J.* **2007**, *13*, 9236–9244. (d) Vargas, A.; Bonalumi, N.; Ferri, D.; Baiker, A. *J. Phys. Chem. A* **2006**, *110*, 1118–1127.

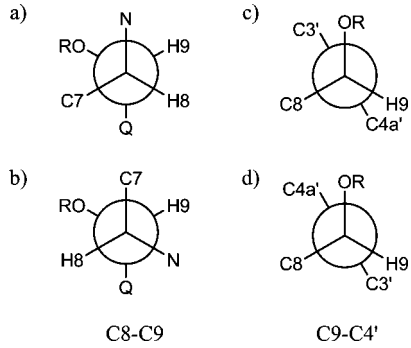

FIGURE 1. Newman projections of conformations of cinchonidine derivatives (Q = quinoline moiety). *Open(3)* conformation is formed by combining the staggered conformation (**a**) along the C8−C9 bond with the conformation (**c**) along the C9−C4′ bond. Analogously, *Closed(1)* = (**b** + **d**); *Closed(2)* = (**b** + **c**); *Open(4)* = (**a** + **d**).

the tilted modifier species in the enantioselection step has also been discussed.[12]

Another elementary feature of the modifier-catalyst system is that the stereochemistry of the main product isomer is determined by modifier configuration.[1] Thus, in the enantioselective hydrogenation of PPD, (*R*)-1-hydroxy-1-phenyl-2-propanone **2** is obtained in excess when cinchonidine is used as the chiral catalyst modifier (Scheme 1).[13] By use of cinchonine, the opposite product enantiomer is formed in excess. When *O*-ether derivatives of cinchona alkaloids are employed as surface modifiers in the hydrogenation of PPD, either the enantioselectivity is inverted or, alternatively, no chiral induction is observed.[5e] Motivated by these structure−selectivity relationships, we decided to investigate in detail the structures and conformational behavior of the cinchona alkaloid *O*-ethers that were earlier evaluated as chiral modifiers in the enantioselective hydrogenation of PPD (Scheme 1).[5e] We demonstrate here that the conformation found to be abundant in the liquid phase has no direct correlation with the enantioselectivity of the PPD hydrogenation reaction.

2. Results and Discussion

2.1. NMR Analysis. In order to correlate the ee's observed in the catalytic experiments (Table 1) with the relative population of any modifier conformation found to be abundant in the liquid phase, four cinchona alkaloid derivatives were analyzed in $CDCl_3$ and toluene-d_8 solutions by dynamic NMR and NOE techniques. For these experiments, the *O*-ether derivatives **4**, **5**, **7**, and *O*-(propyldimethylsilyl)-10,11-dihydrocinchonidine (PDMSODHCD, **13**) were selected. The last mentioned modifier is obtained by hydrogenation of both the allyl and vinyl groups of *O*-(allyldimethylsilyl)cinchonidine (**8**). The structures of these two *O*-silyl ether modifiers (**7** and **8**) resemble each other and, after hydrogenation of the C═C double bonds during the first minutes of the reaction, differ only by the alkyl chains attached to the silicon atom. Enantioselectivity of the PPD hydrogenation over the catalyst modified by **7** is different from that over the catalyst modified by **8**. When the former was used as modifier,

TABLE 1. Enantiomeric Excess (ee) Observed in the Hydrogenation of 1-Phenyl-1,2-propanedione (PPD, 1) over Pt/Al_2O_3 Catalyst Modified with Cinchona Alkaloid *O*-Ethers

modifier	ee[a] (%)
MeOCD (**4**)	10 (*S*)-**2**[b]
PhOCD (**5**)	28 (*S*)-**2**[b]
TMSOCD (**6**)	0
TBDMSOCD (**7**)	27 (*S*)-**2**[b]
ADMSOCD (**8**)	1 (*S*)-**2**[b]
DPMSOCD (**9**)	3 (*S*)-**2**[b]
MeOCN (**10**)	32 (*R*)-**2**[b]
PhOCN (**11**)	33 (*R*)-**2**[b]
TMSOCN (**12**)	30 (*R*)-**2**[b]
PDMSODHCD (**13**)	1 (*S*)-**2**[b,c]

[a] ee = {[(*R*)-**2**] − [(*S*)-**2**]}/{[(*R*)-**2**] + [(*S*)-**2**]} at 50% conversion of PPD. [b] Configuration of the major product enatiomer. [c] Same as obtained for ADMSOCD (**8**). ADMSOCD (**8**) under hydrogenation conditions is rapidly converted to PDMSODHCD (**13**).

a substantial inversion of enantioselectivity was observed and the (1*S*)-hydroxyketone **2** was produced after the first hydrogenation step with enantiomeric excess of approximately 28%.[5e] In the case of **8**, enantioselection was not observed. Compound **5**, although structurally unrelated to **7**, exhibits a very similar behavior as chiral modifier in the hydrogenation of PPD, whereas **4** favors the production of (1*S*)-hydroxyketone with enantiomeric excess of approximately 10%.[5e]

In solutions, cinchona alkaloids exist as mixtures of conformations that are in rapid equilibria at room temperature. Therefore, averaged signals are observed by NMR spectroscopy. Conclusions concerning the conformational behavior of CD have previously been drawn from spectral data acquired at room temperature.[6a–c] In this case, the calculations of conformer populations are limited to two-site exchange,[14] whereas for cinchonidine in solution at least three conformations were observed by NOE. Nevertheless, some approximations allow estimating the contribution of *Open(3)* conformation while not describing the other counterparts.[6a] In order to extract the complete data on conformational behavior, at least one conformation should be separated, e.g., by freezing the equilibria at low temperature. Unfortunately this approach could not be applied to parent cinchona alkaloids in nonpolar solvents due to their poor solubilities[15] at ambient and in particular at low temperatures. Solubilities of the cinchona alkaloid *O*-ether derivatives are, however, remarkably improved and enable the discrimination of signals arising from the individual conformers. Accordingly, separation of the average signals has been observed earlier for **4** in $CD_2Cl_2/CDCl_3$ at low temperature.[6a]

2.1.1. *O*-Methylcinchonidine (4). The conformational equilibria of **4** were studied in toluene-d_8 and $CDCl_3$ using NMR spectroscopy. When the temperature of the sample was gradually decreased, the signals were first broadened and coalescence was achieved at approximately −30 °C (Figure 2). When the temperature was lowered below the coalescence, two sets of signals could be observed. The signals from these conformations were most sharpened at −70 °C in a ratio of 85:15 in toluene-d_8. A coupling constant $^3J_{H8,H9}$ of approximately 9.8 Hz was observed for the minor conformation. Assignment of the conformations was based on NOE analysis at −70 °C. A

(10) (a) Nieminen, V.; Taskinen, A; Toukoniitty, E.; Hotokka, M.; Murzin, D. Yu. *J. Catal.* **2006**, *237*, 131–142. (b) Taskinen, A.; Nieminen, V.; Hotokka, M.; Murzin, D. Yu. *J. Phys. Chem. C* **2007**, *111*, 5128–5140.

(11) Ma, Z.; Lee, I.; Zaera, F. *J. Am. Chem. Soc.* **2007**, *129*, 16083–16090.

(12) (a) Jeffery, E. L.; Mann, R. K.; Hutchings, G. J.; Taylor, S. H.; Willock, D. J. *Catal. Today* **2005**, *105*, 85–92. (b) Busygin, I.; Tkachenko, O. P.; Nieminen, V.; Borovkov, V. Yu.; Sillanpää, R.; Toukoniitty, E.; Murzin, D. Yu.; Kustov, L. M.; Leino, R *J. Phys. Chem. C* **2007**, *111*, 9374–9383.

(13) Toukoniitty, E.; Mäki-Arvela, P.; Kuzma, M.; Villela, A.; Neyestanaki, A. K.; Salmi, T.; Sjöholm, R.; Leino, R.; Laine, E.; Murzin, D. Yu. *J. Catal.* **2001**, *204*, 281–291.

(14) Sandstrom, J. *Dynamic NMR Spectroscopy*; Academic Press: London, 1982; p 19.

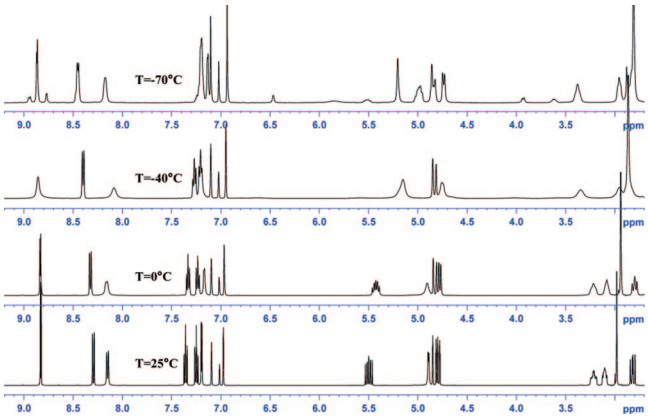

FIGURE 2. ^{1}H NMR spectra of **4** at various temperatures in $CDCl_3$.

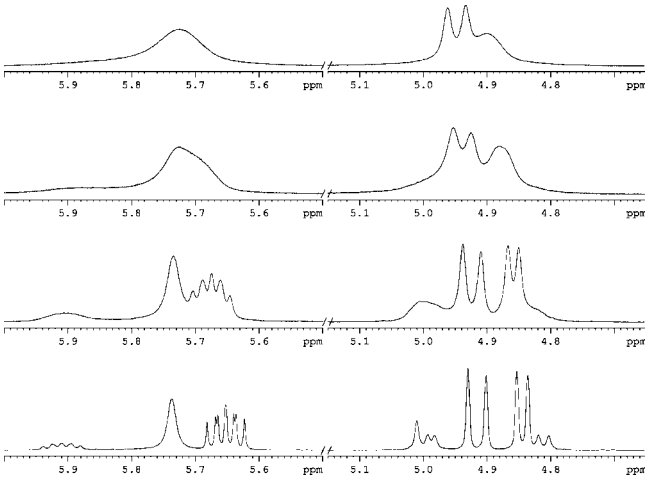

FIGURE 3. Expansion of the ^{1}H NMR spectra of **7** in $CDCl_3$ at different temperatures. From top to bottom: 50, 40, 25, and 5 °C.

characteristic correlation between the H-5′ and H-8 protons (Figure S1, Supporting Information) was observed for the major conformation allowing to assign it as *Open(3)*. The minor conformation could be assigned to *Closed(1)*, as confirmed by the strong NOE between H-3′ and H-9. A weak correlation was also found between H-3′ and H-8 for the major set of the signals, indicating that *Closed(2)* might have some contribution in the equilibrium. In $CDCl_3$, *O*-methylcinchonidine **4** exhibits a similar conformational behavior as in toluene-d_8. The ratio between the major and minor forms was 88:12.

2.1.2. *O*-(*tert*-Butyldimethylsilyl)cinchonidine (7). The ^{1}H NMR spectra of **7** at different temperatures reveal conformational equilibria in solution (Figure 3). Two sets of signals were observed already at room temperature in the ratio of 80:20 in $CDCl_3$ and 71:29 in toluene-d_8. The coalescence point could be reached by heating the sample to 50 °C, whereas for **4** separation of the average signals was observed at −30 °C. Hence, the interconversional barrier for **7** with a bulkier group at C(9) is higher than for **4**. Two sharp signals from H-9 could clearly be separated at 5 °C: a major broad singlet at 5.74 ppm and[16] a minor doublet at 4.81 ppm with $^3J_{H8,H9} = 9.6$ Hz. The broad singlet can be assigned to the *Open(3)* conformation in which the dihedral angle H−C(9)−C(8)−H is close to −90° and the proton−proton coupling is small as suggested by the Karplus equation. The broadening of this signal results from

(15) Ma, Z.; Zaera, F. *J. Phys. Chem. B* **2005**, *109*, 406–414.

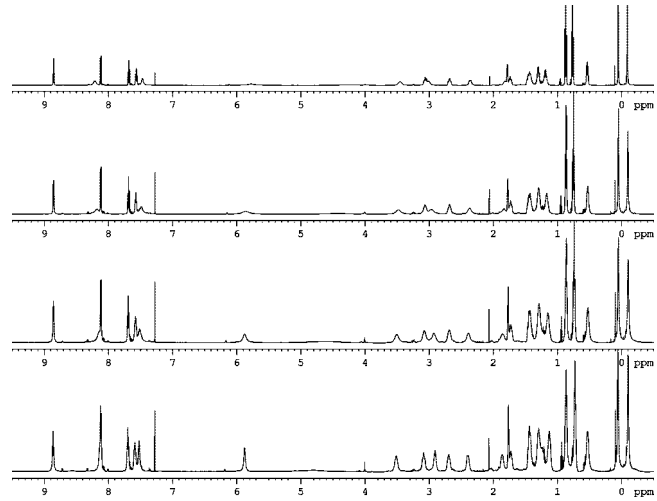

FIGURE 4. ^{1}H NMR spectra of **13** at different temperatures. From top to bottom: 40, 25, 15 and 5 °C.

the closed conformations involved in the equilibria. When the signal at 5.74 ppm was irradiated in an NOE difference experiment at room temperature, two negative peaks, at 5.74 and 4.81 ppm, were observed indicating transfer of magnetization to the minor conformer, which is in rapid equilibrium with the major one. The 1D selective NOESY experiments were performed at −50 °C in $CDCl_3$ solution in order to freeze the equilibria and to assign the individual conformers. The following NOEs were observed by irradiation of H-9 of the major conformation: a strong NOE with H-5′, a weak NOE with H-8 and a weak NOE with H-6b (proton designations and the proton−proton distances for different conformers of **7** are available as Supporting Information). When the H-5′ of the major conformation was irradiated, a strong NOE with H-9 and a weak NOE with H-8 were observed. The irradiation of H-3′ revealed NOE between H-3′ and H-7b and a weak correlation between H-3′ and H-8. These NOEs are indicative of the major set of the ^{1}H NMR signals being a mixture of *Open(3)* and *Closed(2)* conformers. The following NOEs were observed for the minor form: a strong NOE from H-9 to H-3′, a moderate from H-5′ to H-8, a weak NOE from H-9 to H-6b and also from H-3′ to H-6b. Hence, the minor conformation was identified as *Closed(1)*.

Remarkably, the complete assignment of the minor group of the signals was performed here for the first time and is provided in the Supporting Information.

2.1.3. *O*-(Propyldimethylsilyl)-10,11-dihydrocinchonidine (13). The ^{1}H NMR spectra of **13** in $CDCl_3$ at different temperatures are represented in Figure 4. The H-9 proton occurs as a broad signal at 5.94−5.75 ppm and as a small hump between 4.8 and 4.0 ppm at room temperature. Upon heating the sample, the H-9 signals, in contrast to the rest of the spectrum, are broadened to a higher extent. The coalescence point was reached at 40 °C. When the sample was cooled down to 5 °C, two sets of signals could clearly be observed. The H-9 signal from the major conformer is sharpening upon cooling. It appears as a broad singlet centered at 5.88 ppm at 5 °C. The signal has the smallest line width at −15 °C and starts to broaden below this temperature. When the sample was cooled to −30 °C in toluene-d_8 solution, H-9 proton of the minor conformer appears as a doublet at 4.76 ppm with $^3J_{H8,H9} = 9.8$ Hz. Irradiation of the H-9 of the major conformer in NOE difference experiments at room temperature turns that of the minor form in a negative

phase indicating rapid exchange between the conformers. The ratio between the two sets of signals is 90:10 in $CDCl_3$ and 85:15 in toluene-d_8. The assignment of the conformers was carried out by measuring the NOE at −70 °C in toluene-d_8. The correlations detected for **13** were similar to those observed for **7** with the exception of the NOE between H-9 and H-6b, which was more pronounced in the case of **13**. This very likely originates from the higher population of *Closed(2)* conformer in the solution of **13** as compared to **7**.

2.1.4. *O*-Phenylcinchonidine (2). The ^{1}H NMR spectra of **2** in both $CDCl_3$ and toluene-d_8 are represented by averaged signals at room temperature. The H-9 proton appears as a broad singlet at 6.10 ppm in $CDCl_3$ and as a doublet at 6.06 ppm in toluene-d_8. Low-temperature experiments at −30 °C in $CDCl_3$ did not alter the ^{1}H NMR spectra, and averaged spectra were again observed. In toluene at −70 °C, the signals were broadened and assignment of the conformers was complicated by spin diffusion. The NOESY spectrum displayed all possible correlations between all protons. Correspondingly, the conformations were assigned in $CDCl_3/CD_2Cl_2$ solution. When the temperature was lowered to −70 °C, two clear sets of signals were observed. The H-9 signal from the minor conformer appeared as a doublet at 5.32 ppm with a coupling constant $^3J_{H8,H9}$ = 10.3 Hz. The population of the minor set was 6% and was assigned as *Closed(1)* conformation on the basis of a strong NOE from H-9 to H-3′. NOE difference spectra in toluene-d_8 and $CDCl_3$ at room temperature revealed a strong NOE between H-9 and H-5′, a moderate NOE between H-3′ and H-7b and a weak NOE between H-9 and H-6b as well as between H-9 and H-8. These NOEs are characteristic of the *Closed(2)* and *Open(3)* conformations. A very weak interaction between H-9 and H-3′, being indicative of *Closed(1)* conformations, was also observed. Since the *Closed(1)* conformer was not separated for **2** in $CDCl_3$ at −30 °C and in toluene-d_8 at −70 °C, quantification of the results is based on the data obtained at room temperature. Exact quantification of the NOE difference results requires information on the ratio of the *Closed(2)* and *Open(3)* conformers in solution as the distances between H-9 and H-5′ are different for the two. Nevertheless, it is possible to estimate the interval in which the population of *Closed(1)* conformation can vary depending on the ratio mentioned above. Taking into account the NOE peak integrals and the distances raised to the sixth power, we obtained the population of *Closed(1)* as being between 8% and 10% in toluene-d_8 and between 13% and 17% in $CDCl_3$.

2.1.5. Conformational Equilibria by Spin Simulation/Iteration. Since the coalescence point for three cinchona alkaloid *O*-ether derivatives decreases in the series **7** > **4** > **5**, the interconversion between the *Closed(1)* and *Closed(2)* should be less hindered for the phenyl derivative **5** than for the methyl derivative **4** and silyl derivative **7**. The interconversion barriers will be assessed theoretically in the next section.

The conformational equilibria of **7** in $CDCl_3$ solution are represented in Scheme 2. Because of their low interconversional barrier,[6a,c] it is not possible to separate the signals of the *Closed(2)* and *Open(3)* conformers, even at low temperatures, and only by resorting to spin simulation/iteration techniques could the ratio of *Closed(2)* and *Open(3)* conformers be reliably extracted. Consequently, the corresponding coupling constants were analyzed by the PERCH software.[17] The results are

SCHEME 2. Conformational Equilibria of 7 in Solution

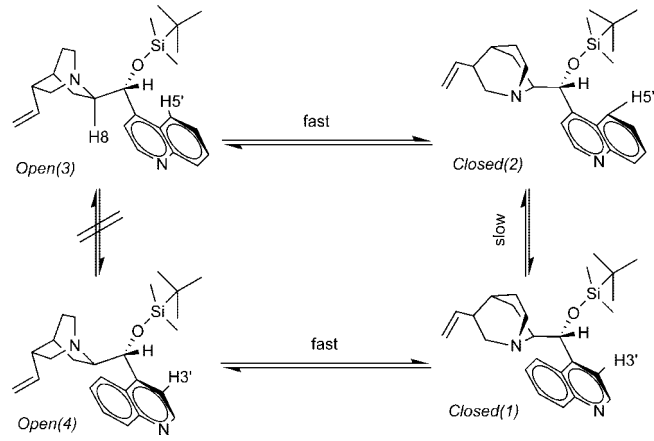

presented in Table 2. A very good agreement between the experimentally recorded and calculated spectra was obtained for **4**, **5**, and **7**, whereas for **13** the reliability of the fit was lower due to signal broadening. Thus, for **13** in toluene-d_8, the coupling constants could not be easily resolved. The torsion angles H−C(9)−C(8)−H were calculated from the Altona equation[18] using the MestRe-J graphical tool.[19] The populations were calculated by confrontation of the derived angle with the angles in optimized structures of *Closed(2)* and *Open(3)* conformers (for details, see Supporting Information).

By summarizing the results, it can be concluded that the *Open(3)* conformation is the most populated in solutions of **7**, **5**, and **4** in toluene-d_8 and $CDCl_3$, whereas for **13** in $CDCl_3$ *Closed(2)* is the predominant conformation.

2.2. Computational Study. The molecular structures and energies of the methyl *O*-ether derivatives **4** and **10**, and the silyl *O*-ether derivatives **7** and **13** were investigated in the gas phase and in solvents ($CHCl_3$, toluene) using density functional theory (DFT) at the B3LYP/T(ON)DZP level. Detailed information on the computational methods employed can be found in Supporting Information.

2.2.1. *O*-Methyl Derivatives of Cinchonidine (4) and Cinchonine (10). The results for **4** and **10** are presented in Table 3. Optimized geometries for the conformations of **4** are visualized in Figure 5. On the basis of the computational electronic energies, *Open(3)* conformation was the most stable one, followed by *Closed(1)* and *Closed(2)* for both *O*-methyl derivatives **4** and **10**. The *Closed(1)* conformers were 4.8 and 4.4 kJ mol^{-1} less stable than the *Open(3)* conformers of **4** and **10**, respectively. The relative Gibbs energies (ΔG) at 25 °C and 1 bar are rather similar to the relative electronic energies. Only slight stabilization of all conformations (except for *Open(5)* of **4**) with respect to *Open(3)* was observed. Thus, *Closed(1)* was stabilized by 1.2 and 2.6 kJ mol^{-1} for **4** and **10**, respectively. When the solvent effects of toluene were taken into account by the conductor-like screening model (COSMO),[20] the *Closed(1)*, *Closed(2)*, *Open(4)*, and *Open(5)* conformations were stabilized further relative to *Open(3)*. According to Boltzmann statistics, the populations of the *Closed(1)* and *Open(3)* conformations of **10** were almost the same, whereas in the case of **4**, the

(16) (a) Karplus, M. *J. Am. Chem. Soc.* **1963**, *85*, 2870–2871. (b) Karplus, M. *J. Phys. Chem.* **1959**, *30*, 11–15.

(17) Laatikainen, R; Niemitz, M; Weber, U; Sundelin, J.; Hassinen, T.; Vepsäläinen, J. *J. Magn. Reson. Ser. A* **1996**, *120*, 1–10.

(18) Altona, C. In *Encyclopedia of NMR*; Grant, D. M., Morris, R., Eds.; Wiley: New York, 1996; pp 4909−4923.

(19) Navarro-Vazquez, A.; Cobas, J.; C.; Sardina, F. J.; Casanueva, J.; Diez, E. *J. Chem. Inf. Comput. Sci.* **2004**, *44*, 1680–1685.

TABLE 2. Populations of Conformers in the Solutions of Cinchona Alkaloid *O*-Ethers and the Efficiencies of the Compounds as Chiral Modifiers in the Hydrogenation of PPD

				Closed(1)		*Closed(2)* and *Open(3)*		
modifier	ee[a]	solvent	*T*, °C	$^3J_{H9,H8}$, Hz	*P*[b], %	$^3J_{H9,H8}$, Hz	$P_{Closed(2)}$[c], %	$P_{Open(3)}$[c], %
13	0[d]	toluene-d_8	−30	9.85	15	n.a.[e]	n.a.	n.a.
		$CDCl_3$	5	n.a.	10	4.50 ± 0.5	48 ±3	42 ±3
4	10 (*S*)-**2**	toluene-d_8	−50	9.84	15	2.50 ± 0.3	29 ±2	56 ±2
		$CDCl_3$	−50	n.a.	12	2.70 ± 0.1	32	56
7	27 (*S*)-**2**	toluene-d_8	0	n.a.	29	3.40 ± 0.1	29	42
		$CDCl_3$	5	9.67	20	2.70 ± 0.1	29	51
5	28 (*S*)-**2**	toluene-d_8	25	n.a.	9 ± 1[f]	3.05 ± 0.1	33 ±1	58 ±1
		$CDCl_3$	0	n.a.	15 ± 2[f]	2.27 ± 0.1	26 ±2	60 ±2

[a] Enantiomeric excess in the hydrogenation of PPD in toluene, taken from ref 5e. [b] Population of the conformer as studied by ^{1}H NMR. [c] Population of the conformer derived from the coupling constant $^3J_{H9,H8}$; ± 1% if not specified. [d] Data for **8**. [e] Not available. [f] Calculated from NOE at room temperature.

TABLE 3. Relative Electronic Energies (Δ*E*), Gibbs Energies (Δ*G*), and Equilibrium Populations (P_B) of the Conformations of 4 and 10

	4		**4** in toluene		**10**		**10** in toluene	
	ΔE^a	ΔG^a	ΔG^a	P_B[b]	ΔE^a	ΔG^a	ΔG^a	P_B[b]
Closed(1)	4.8	3.6	2.5	22	4.4	1.8	0.3	46
Closed(2)	7.2	4.9	3.3	16	10.9	9.1	6.9	3
Open(3)	0.0	0.0	0.0	60	0.0	0.0	0.0	51
Open(4)	10.4	9.0	8.8	2	15.2	13.6	13.5	0
Open(5)	22.1	24.1	21.7	0	20.9	20.4	17.8	0

[a] In kJ mol^{-1}. [b] Equilibrium population of conformation according to Boltzmann statistics, %.

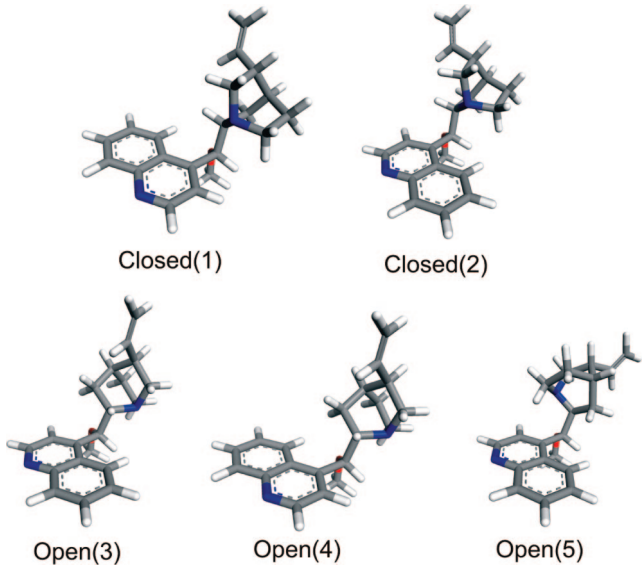

FIGURE 5. Conformations of **4** optimized at the B3LYP/T(ON)DZP level of theory.

population of *Closed(1)* was about one-third of the population of *Open(3)*. Accordingly, *Closed(1)* was just 0.3 kJ mol^{-1} less stable than *Open(3)* for **10** in toluene. *Closed(2)* of **10** was always at least 5 kJ mol^{-1} less stable than *Closed(1)*.

2.2.2. *O*-Silyl Derivatives of Cinchonidine. The optimized structures of the conformations of **7** (Figure S3) and the most relevant NOE proton−proton distances (Table S2) are provided as Supporting Information. The stabilities of the conformers and their equilibrium populations according to Boltzmann statistics are given in Table 4. On the basis of the computational electronic energies, *Open(3)* is the most abundant conformation (69% proportion) followed by *Closed(1)* and *Closed(2)*. The silyl ether derivatives of cinchonidine have additional rotational degree of freedom due to the substituent at the C(9)-O position. Starting from the most stable *Open(3)* conformation of **7**, rotation around the O-Si bond yields a shorter distance between H-9 and $SiC(CH_3)$, increasing the electronic energy by 7.5 kJ mol^{-1}. This indicates increased steric hindrance due to the bulky *tert*-butyl group. The equilibrium population of the *Closed(2)* conformation (11% proportion) is approximately the same as that of *Closed(1)* (19% proportion). Only traces of two other studied conformations, namely, *Open(4)* and *Open(5)*, are expected to be involved in the equilibria for **7** as they are less stable than the dominating *Open(3)* conformation. Accordingly, the three most abundant conformations of **13** were studied. The results obtained for **13** are similar to those for **7**. *Open(3)* (73% proportion) is the most populated conformation for **13** according to the electronic energies. However, the ee's obtained in the hydrogenation of **1** over the catalysts modified by these two silyl *O*-ether derivatives are different (Tables 1 and 2).[5e] Therefore, it can be concluded that the inversion of enantioselectivity in the specific case studied in this work cannot be rationalized by considering the electronic energies of the conformers in the gas phase only.

Solvent effects on the conformational equilibria of **7** were also studied by the COSMO model.[20] Stabilization of the closed conformations relative to *Open(3)* was observed when the effect of apolar solvents chloroform and toluene was considered. Boltzmann equilibrium populations obtained from the DFT calculations are supported by the NMR data (cf. Tables 2 and 4). The small deviations between the experimental and theoretical values can be attributed to the inaccuracy of COSMO when treating the screening effects of nonpolar solvents. The absolute error in the energies resulting from the evaluation of the screening effects is typically less than 4 kJ mol^{-1} when the dielectric constant of the solvent is low ($\epsilon \approx 2$). Nevertheless, the computational results are well in line with the experimental values and demonstrate the applicability of the approach utilized in this work for studying such complex systems.

The Gibbs free energies including the solvent effects of toluene and chloroform were also computed for the three most stable conformations of **7**. Relative stabilities of the conformers with respect to the stabilities based on gas phase electronic energies changed notably. In fact, the results were rather surprising. According to the Gibbs energies, the most stable conformation in the gas phase was *Closed(2)*. The *Open(3)* and *Closed(1)* conformations were less stable than *Closed(2)* by 1.6 and 2.7 kJ mol^{-1}, respectively. In toluene and chloroform, *Closed(1)* was the most stable conformation while the *Closed(2)* and *Open(3)* conformers were less stable by 1.1−3.4 kJ mol^{-1}.

TABLE 4. Relative Electronic Energies (Δ*E*), Gibbs Energies (Δ*G*), and Equilibrium Population (P_B) of the Conformations of 7 and 13

	7				**7** in $CHCl_3$				**7** in toluene				**13**	
	ΔE^a	$P_B{}^b$	ΔG^a	$P_B{}^b$	ΔE^a	$P_B{}^b$	ΔG^a	$P_B{}^b$	ΔE^a	$P_B{}^b$	ΔG^a	$P_B{}^b$	ΔE^a	$P_B{}^b$
Closed(1)	3.2	19	2.7	18	1.8	27	0.0	66	2.4	24	0.0	48	3.7	17
Closed(2)	4.5	11	0.0	54	3.1	16	3.4	17	3.6	14	2.1	21	4.8	11
Open(3)	0.0	69	1.6	29	0.0	56	3.4	17	0.0	61	1.1	31	0.0	73
Open(4)	11.0	1			10.5	1			10.7	1				
Open(5)	20.2	0			20.1	0			20.2	0				

[a] In kJ mol^{-1}. [b] Equilibrium population of conformation according to Boltzmann statistics, %.

Instead, *Open(3)* was the most stable conformer in the gas phase and in solution according to the electronic energies. Such a large difference between the relative Gibbs energies and electronic energies, not observed in the cases of **4** and **10**, could be explained by the low-frequency vibrations of **7** which are most poorly described by the harmonic oscillator approximation. Small errors in very small nonzero frequencies can lead to very large errors in entropies and, consequently, in the Gibbs energies.[21] Therefore, it may be better to restrict oneself to discuss only enthalpy or internal energy. Consequently, the enthalpy energies for **7** are presented in Supporting Information (Table S3). The results show that the computational values of the relative enthalpies are similar to those of the relative electronic energies.

2.2.3. Rotational Barriers. The potential energy map for **6** was earlier scanned at the HF/3-21G level of theory.[6d] It was found that the *Closed(1)* conformation has practically the same energy as *Open(3)*. The interconversion between *Open(3)* and *Open(4)* does not take place as a result of the high energy barrier. The interconversion between *Closed(1)* and *Closed(2)* was also hampered when compared to cinchonidine. It is interesting that this path has a saddle point energy of 44 kJ mol^{-1}. Baiker an co-workers have studied the conformational behavior of *O*-phenylcinchonidine **5** by scanning the potential energy surface using the semiempirical PM3 Hamiltonian and optimizing the minimum energy conformations at the DFT-B3LYP/6-31G(d,p) level.[9d] It was found that the structural and energetic data for **5** is rather similar to that for the parent compound cinchonidine. Here, we aimed to investigate the influence of the substituent bulkiness on the rotational barriers by DFT. The interconversions *Closed(1)*−*Closed(2)* and *Open(3)*−*Open(4)* for **4**, **7**, and **5** as well as *Closed(2)*−*Open(3)* for **4** were studied.

The energies of the optimized *Closed(1)* and *Closed(2)* conformations together with the transition state conformations are represented in Figure 6 as a function of the C3′−C4′−C9−C8 torsional angle (τ_1, for definition and direction of the rotation see Supporting Information). Interconversion between the *Closed(1)* and *Closed(2)* conformations has the lowest energy barrier for **5** (30 kJ mol^{-1}) and the substituents could be arranged by the rotational hindrance in the following order: TBDMS (**7**) > Me (**4**) > Ph (**5**). The lowest energy barrier observed for compound **5** is very well in line with the NMR results and could be explained by the flat geometry of the phenyl ring. Indeed, in the transition state structure of **5**, the distances between the quinuclidine moiety and the *O*-substituent and between the aromatic moiety and the *O*-substituent are 2.69 and 2.43 Å, respectively, whereas in the case of **4**, both distances are shorter (ca. 1.90 Å). Therefore, the rotation around the C4′−C9 bond is more hindered for **4** than for **5**.

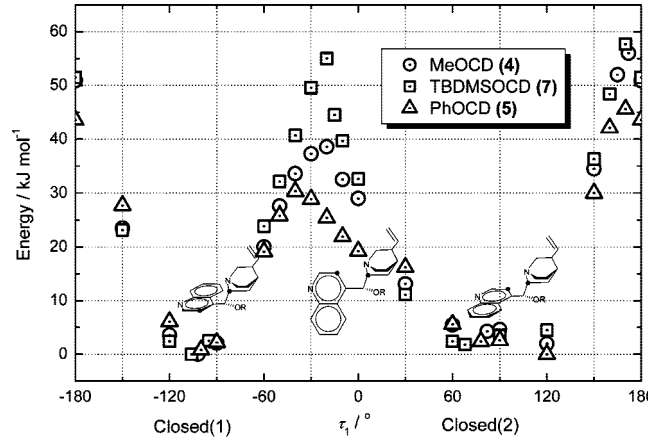

FIGURE 6. Energy of *Closed(1)*−*Closed(2)* interconversion for **4**, **7**, and **5**.

The influence of direction for the quinoline moiety rotation was also investigated. It was found that "the substituent site" rotation (in the direction of τ_1 increase for *Closed(1)* → *Closed(2)* interconversion and in the direction of τ_1 decrease for the reversed process) is energetically preferred over "the quinuclidine site" rotation for **4** and **5**, whereas for **7**, both directions are rather equal. The energy of "the quinuclidine site" barrier did not depend on the size of the tetragonal *O*-substituent (58 kJ mol^{-1} for both **4** and **7**). However, this barrier was slightly lower for the flat phenyl ring. Most likely, it was originated from the minor repulsion between H-3′ and *O*-substituent, which was lower for **5** in the same manner as reasoned earlier for the H5′-R-H7b repulsion.

During the optimization of the molecular geometries with τ_1 fixed to 120°, it was found that energies of the obtained structures are lower than energies of the *Closed(2)* conformers for **4** and **5** (Figure 6). The close inspection of the geometries revealed steric repulsions between the quinuclidine-*N* and H-5′ which force the structures to change their τ_2 angles by approximately 80° in the direction toward open conformation. When the τ_1 angle was further increased to 150°, the steric repulsion between H-5′ and H-8 forced backward change of τ_2 to the values characteristic for closed conformations.

The energies of *Open(3)*↔*Open(4)* interconversion barriers are represented in Figure 7. The correlation for *Open(3)* ↔ *Open(4)* interconversion was similar to that for *Closed(1)* ↔ *Closed(2)* interconversion. Compound **5** had the lowest and compound **7** had the highest energy barriers for both *Open(3)* → *Open(4)* and the reversed processes. Generally, the *Open(3)* ↔ *Open(4)* interconversions were less favorable than *Closed(1)* ↔ *Closed(2)* interconversions. Therefore, equilibria in the solutions of **7** could be described as represented in Scheme 2, whereas in solutions of **5**, the *Open(3)* ↔ *Open(4)* interconversion is rather fast in the NMR time scale.

(20) Klamt, A.; Schüürmann, G. *J. Chem. Soc., Perkin Trans. 2* **1993**, 799–805.

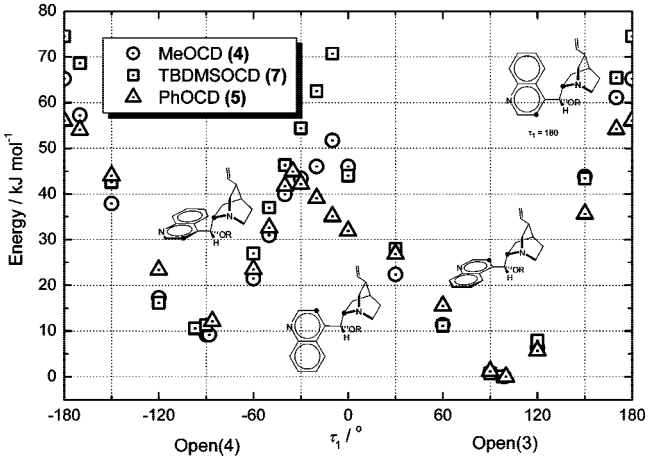

FIGURE 7. Energy barrier of *Open(3)*−*Open(4)* interconversion for **4**, **7**, and **5**.

It is noteworthy that the NMR results are very much in line with the data on the rotational barriers as studied by DFT. *Closed(1)* conformation of the *O*-silyl ethers was observed by ^{1}H NMR as a separate set of signals in $CDCl_3$ and toluene-d_8 at room temperature, whereas it was detected for **4** at −30 °C and for **5** only at −70 °C. Computational study of the influence of the substituent bulkiness on the rotational barriers showed the increase of the hindrance for interconversion between *Closed(1)* (the minor set of the signals in NMR spectra) and *Closed(2)* (component of the major set of the signals in NMR spectra) within the same series: **7** (55 kJ mol^{-1}) > **4** (39 kJ mol^{-1}) > **5** (30 kJ mol^{-1}).

Since it was not possible to separate the *Closed(2)* and *Open(3)* conformers at low temperature, we have also calculated the energy barrier of this interconversion for compound **4**. The interconversion barrier between *Closed(2)* and *Open(3)* is expected to be 13−17 kJ/mol as studied by Bürgi and Baiker[6a] with model compounds, and consequently, the conformational equilibria between *Closed(2)* and *Open(3)* could not be frozen at −90 °C. As illustrated in Supporting Information (Figure S4), the energy barrier for *Open(3)* → *Closed(2)* transfer was 11 kJ mol^{-1}, whereas it was only 2.5 kJ mol^{-1} for the reversed process. These data are in line with the results obtained earlier by Bürgi and Baiker.[6a]

2.3. X-Ray Structures of the Modifiers. In a recent paper, Zaera and coauthors[11] studied the adsorption of cinchona alkaloids onto the platinum surface from solutions of different alkaloid concentrations. It was determined that, at saturation coverage, the quinoline ring of cinchonidine tilts along its longitudinal axis to optimize $\pi-\pi$ intermolecular interaction. Moreover, it was suggested that intermolecular $\pi-\pi$ stacking is a dominant force defining the adsorption geometry. Since a similar stacking defines the crystal lattice in the solid,[22] the modifier crystal structures gain an additional value. Thus, in the light of these results it would be interesting to compare the potential intermolecular $\pi-\pi$ stacking in different derivatives of cinchona alkaloids.

Crystal structures of three cinchona alkaloid derivatives, *O*-methylcinchonidine (**4**), *O*-phenylcinchonidine (**5**), and *O*-methylcinchonine (**10**), were determined in the present study.[23] Regarding the interesting behavior of the cinchona alkaloid

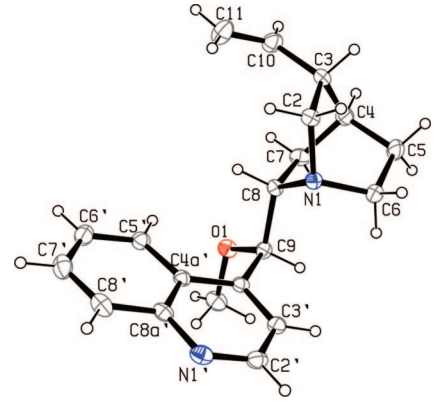

FIGURE 8. Molecular structure of **4**.

TABLE 5. (a) Calculated Dihedral Angles for Several Conformers of Cinchonidine and (b) Experimental Dihedral Angles of Modifiers in the Solid State

(a) CD[6a]	*Closed(1)*	*Closed(2)*	*Open(3)*	*Open(4)*	*Open(5)*
τ_1[a]	−107.0	80.4	101.4	−89.3	85.7
τ_2[b]	−176.8	−172.5	−78.3	−77.5	76.2
N(1)−C(8)−C(9)−C(4′)	57.5	65.3	153.6	150.1	−48.6

(b)	CD[22]	**4**	**5**	CN[24]	**10**
τ_1	101.5(7)	−106.2(3)	88.9(5)	−99.82	102.5(2)
τ_2	−70.8	175.6	−72.3	70.8	173.7
N(1)−C(8)−C(9)−C(4′)	158.0(6)	52.7(3)	162.6(4)	−160.35	−59.0(3)

[a] τ_1: C(3′)−C(4′)−C(9)−C(8). [b] τ_2: H(9)−C(9)−C(8)−H(8).

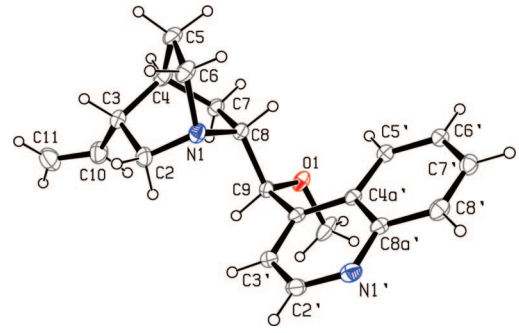

FIGURE 9. Molecular structure of **10**.

O-ethers as chiral modifiers, the study of their structures in crystal form may provide additional information relevant to the structures of these molecules on the surface. Molecular structures of these compounds are represented in Figures 8–10. By analyzing the data in Table 5 and Table S1 (Supporting Information), it is clear that the *O*-methyl ether derivatives adopt the *Closed(1)*-like conformation, whereas **5** adopts the *Open(3)*-like conformation in the crystal. Since the positions of hydrogen atoms are generated by calculations from the positions of the host carbon atoms, the estimated deviation of the dihedral angle τ_2 could be in the order of 2−3°. Therefore, we additionally provide here the N(1)−C(8)−C(9)−C(4′) dihedral angles with standard deviations for the parameter.

It is noteworthy that geometries of the optimized conformations are slightly different from those in the crystal. Consequently, the dihedral angles τ_1 and τ_2 for **5** in the crystal differ by 12° and 8° from the minimum energy *Open(3)* conformation

(21) Cramer, C. J. *Essentials of Computational Chemistry - Theories and Models*; Wiley: Chichester, 2002; p 340.
(22) Oleksyn, B. J. *Acta Crystallogr.* **1982**, *B38*, 1832–1834.
(23) The X-ray structure of MeOCN has been reported earlier in an independent study: Exner, C. Ph.D. Thesis, University of Basel, 2002.

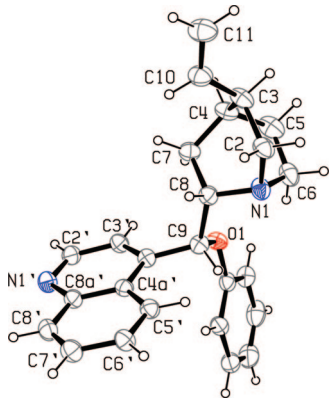

FIGURE 10. Molecular structure of **5**.

optimized by Baiker and co-workers.[9d] However, the relative position of the phenyl ring, which could be defined by the C(9)−O−C_{ipso}−$C_{ortho'}$ dihedral angle differs only by 4° (DFT, 9.9°; X-ray, 5.6°). For *O*-methyl derivatives **4** and **10**, the difference between the dihedral angles in solid and in the gas phase is less and varies from 1° to 2.5°.

Conclusively, due to the bulky *O*-ether substituent, none of the cinchona alkaloid *O*-ether derivatives studied in this work showed $\pi-\pi$ stacking in the crystal. Only weak C···C interactions in two compounds were observed: one in compound **5** (the C···C distance is 3.377(7) Å) and two in **10** (the C···C distances are 3.356(4) and 3.468(4) Å). Possibly, the effect of lateral interactions between molecules could be an important factor in their assembly on the metal surface at relatively high coverages.

2.4. Conformational Equilibria versus Enantioselectivity. The *Open(3)* conformation of cinchonidine has commonly been accepted to have a crucial role in obtaining high enantioselectivity in the hydrogenation of carbonyl compounds over cinchona alkaloid modified platinum catalysts.[6a] The decrease of ee for *O*-substituted cinchona alkaloids in enantioselective hydrogenation of ethyl pyruvate in apolar solvents was related to the population of the *Open(3)* conformation in the liquid phase and consequently on the metal surface.[6a] As a result of modifier adsorption−desorption processes, the conformational equilibria in solution can provide some valuable information on the distribution of the adsorbed species.

Although the conformational equilibria of the parent cinchona alkaloids in the liquid phase have been studied in detail earlier,[6a–c] only a few studies have addressed the conformational behavior of the ether derivatives.[6b,9] The conformations of *O*-phenylcinchonidine **5** have been analyzed by a theoretical-experimental approach.[9d] It was found that *Open(3)* is the predominant conformation in apolar solvents with a fraction of *Closed(2)* conformation, and the population of the latter is in direct proportion to the solvent polarity. Correlation between the inversion of enantioselectivity in ketopantolactone hydrogenation when **5** was used as a chiral modifier and the conformational behavior of **5** and cinchonidine was not observed, as for both alkaloids *Open(3)* is the dominant conformation in $CHCl_3$. *Closed(1)* conformation was omitted from the discussion on the basis of the calculated and experimental VCD spectra confrontation. In the present work, we have demonstrated the involvement of *Closed(1)* conformation of **5** in the liquid phase equilibria by NMR spectroscopy.

(24) Oleksyn, B.; Lebioda, L.; Ciechanowicz-Rutkowska, M. *Acta Crystallogr.* **1979**, *35*, 440–444.

Dijkstra and co-workers studied the conformational equilibria of *O*-methyl-10,11-dihydroquinidine in different solvents.[6b] This compound predominantly adopts the *Open(3)* conformation in $CDCl_3$ and to a lesser amount the *Closed(2)* conformation. *Closed(1)* conformer was not detected. *O*-Methylcinchonidine **4** was studied in $CDCl_3/CD_2Cl_2$ solution at low temperatures by Baiker and co-workers.[6a] In their study, *Closed(1)* conformer was separated at low temperature with a population of 6−7%.

Considering that the modification of the cinchona alkaloid structure induces changes in the conformational equilibria,[6b,c] it was challenging to investigate whether the enantioselectivity over the cinchona alkaloid *O*-ether modified metal catalysts correlates with the population of *Open(3)* or any other conformation in the liquid phase.

The crucial role of the C(9)-OH group of modifiers in enantiodifferentiation over the metal catalyst is incontestable in the hydrogenation of **1**.[5d,e] Under optimal conditions, the main product, (*R*)-**2** (Scheme 1), can be obtained in 65% ee using cinchonidine as the chiral catalyst modifier. When *O*-methyl, *O*-phenyl or *O*-silyl ether derivatives of cinchonidine are used, a loss (ee = 0%) or inversion of enantioselectivity results with 10−28% ee of (S)-2 produced. The same trend is observed with cinchonines as chiral modifier. With parent cinchonine, the main product (*S*)-**2** (Scheme 1) is obtained in 19% ee. When *O*-methyl, *O*-phenyl or *O*-silyl ether derivatives of cinchonine are used, an inversion of enantioselectivity results with (*R*)-**2** being produced in 28−33% ee (Table 1).

After changing the chiral pocket by utilization of cinchona alkaloid *O*-ethers as modifiers, the polar hydroxyl group is replaced by an apolar and bulkier ether group. The modifier−reactant interaction is generally composed of both attractive and repulsive interactions which play a role in the enantiodifferentiating interactions. It is interesting that the new chiral pocket induces the production of the opposite product enantiomer in excess. At first glance, since the attractive interactions (possible H-bonding between the OH-group in the modifier and the carbonyl group in the reactant)[5d] are now replaced by repulsive ones, it would be natural to expect an inversion in the sense of enantioselectivity. In this case one should expect an inversion of enantioselectivity always when the parent cinchona alkaloid is substituted by its *O*-ether. On the contrary, we observe the inversion of enantioselectivity for **4**, **5**, and **7** in toluene, whereas in the same solvent, the modification of the surface with **6**, **8**, and **9** results in the production of a mixture of the product enantiomers in nearly equal amounts.[5e] In the present work, thus, an attempt to correlate the enantioselectivities observed with **8**, **4**, **7**, and **5** (increase in the production of (*S*)-enantiomer within this series) with their conformational equilibria in solution was made. The hydroxyl group of all of these cinchona alkaloid derivatives is blocked by substituents and, therefore, one would not at first hand expect significant differences in their binding to the heterogeneous catalyst surface, as is the case with the parent cinchona alkaloids versus their *O*-ether derivatives.

One of the representatives from each group with similar structure and different properties (**7** and **8**) as well as with different nature of the substituent but similar properties (**7** and **5**) were selected and analyzed by NMR. The results presented in Table 2 demonstrate that direct correlation between the liquid phase populations of conformers in $CDCl_3$ and toluene-d_8 with enantioselectivities in PPD hydrogenation cannot be established. The only possible link to the catalytic data is that the *Open(3)* conformer of **13**, contrary to all the other modifiers studied by

NMR, is not the most representative one in $CDCl_3$ solution and this compound does not induce enantioselectivity in the hydrogenation of **1**. It seems that the modifier adsorption behavior is a midpoint in the enantioselection process. Particularly, the modifier may change the conformation upon adsorption onto the metal surface or, alternatively, the population of a certain conformer on the metal surface is not necessarily correlated with the same in the liquid phase.

In several mechanistic models,[7] it is commonly assumed, while not yet experimentally confirmed, that the origin of enantioselectivity in the Orito reaction is related to the specific interaction between the surface *Open(3)* conformation of the modifier and the reactant. In a paper by Bürgi and Baiker,[6e] a correlation between the liquid phase fraction of *Open(3)* conformation of cinchonidine in different solvents and the enantioselectivities of ketopantolactone hydrogenation over cinchonidine-modified Pt was reported. This observation generally confirms the validity of the Langmuir adsorption equation in this particular case, i.e., that the coverage or adsorption of molecules on a solid surface corresponds to the concentration of these molecules in the liquid phase at a fixed temperature. In the present study, it is demonstrated for the first time that concentrations of any conformers in the liquid phase do not correlate with the fractions of the corresponding surface adsorbed species. The observed phenomenon suggests a more complex dependence of the surface coverage on enthalpy of adsorption.

Recently, Baiker and co-workers,[9c] by means of theoretical calculations and infrared spectroscopic techniques, clearly demonstrated that compound **6** preferentially adsorbs on the platinum surface in surface-quinuclidine-bound mode. These results generally overcome the earlier suggested correlation between the population of conformer in the liquid phase and the observed enantioselectivities in the hydrogenation of α-keto esters[6a] or limit it to the cinchonidine case alone, and are in line with our current findings. Yet compound **4**, as reported,[9c] exhibits an adsorption behavior similar to the parent cinchonidine. These data well describe the features of α-keto ester hydrogenation, while being unable to correlate with the results observed in the hydrogenation of PPD.[5e] DFT calculations are not able to correctly model the noncovalent part of the interaction with the surface. Hence, very little emphasis should be placed on literature conformational data obtained using DFT calculations. Similarly, while vibrational studies of adsorbed alkaloids can give reliable information on the quinoline orientation, it is very doubtful whether they can be used to establish the conformation of the adsorbate. This remains an extraordinarily difficult challenge for surface spectroscopy. A closer inspection is therefore needed regarding the modifier adsorption mode and conformation on the catalyst surface and their role in the enantiodifferentiation process.

3. Conclusions

The complete assignment of the conformational equilibria of the solute cinchona alkaloid *O*-ether derivatives was performed for the first time. In the earlier studies of cinchonidine in solutions, the population of the *Open(3)* conformation was based on an NOE-derived value, whereas the data presented here is based on a more accurate coupling constant analysis. Direct measurements of the population of *Closed(1)* conformation were performed by examination of the NMR spectra at temperatures under conditions of slow exchange on the NMR time-scale. The $^3J_{H8,H9}$ coupling constants of the averaged *Open(3)* and *Closed(2)* conformations were extracted by spin simulation/iteration techniques, and the distribution between these conformations was subsequently calculated from the Altona equation. *Closed(1)* conformation of the *O*-silyl ethers was observed by ^{1}H NMR as a separate set of signals in $CDCl_3$ and toluene-d_8 at room temperature, whereas it was detected for *O*-methylcinchonidine (**4**) and *O*-phenylcinchonidine (**5**) only at low temperatures (−30 and −70 °C, respectively). *Open(3)* was found to be the most populated conformation of **4**, **10**, **7**, and **5** in both $CDCl_3$ and toluene-d_8 by NMR, whereas the population of the *Closed(2)* conformation of **13** was slightly higher than that of *Open(3)* in $CDCl_3$. Populations of the conformers of *O*-methyl derivatives **4** and **10** in toluene and those of **7** in chloroform and toluene were calculated by DFT. The results are in accordance with the experimental data. X-ray structures of **4** and **5** were reported here for the first time. It was observed that the *O*-methyl ether derivatives of cinchonidine **4** and cinchonine **10** adopt the *Closed(1)* conformation in the crystal, whereas *O*-phenylcinchonidine **5** attains the *Open(3)* conformation.

The enantioselectivity over the cinchona alkaloid *O*-ether modified metal catalysts was confronted with the populations of *Closed(1)*, *Closed(2)*, and *Open(3)* conformations in the liquid phase. Thereby, we have demonstrated that the modifier conformation in the liquid phase has a minor role in determining the enantioselectivity in the hydrogenation of PPD over cinchona alkaloid modified platinum catalysts. The driving force for production of one of the enantiomers in excess over another is deduced to result from a specific adsorption of the modifier on the catalyst surface, a phenomenon that does not correlate with the population of the conformers in the liquid phase as was assumed earlier. In other words, the data presented here confirm that the origin of chiral switch phenomenon in the hydrogenation of PPD is related to depletion of the H-bonding interaction between the modifier OH-group and the carbonyl group of the reactant rather than to a decreased population of the *Open(3)* conformation in the solutions of *O*-ether derivatives when compared with the solution behavior of the parent alkaloid.

Additionally, we propose that the method applied here for the complete assignment of conformational behavior of cinchona alkaloid *O*-ethers in solutions might be successfully utilized for correlating the catalyst structure effects with selectivities of different cinchona alkaloid-catalyzed organic reactions.

Finally, as overviewed in the Introduction, conformational equilibria in the solutions of cinchona alkaloids and their derivatives are of interest not only for researchers working in the field of chiral modification of metal catalysts but for broader audiences as well working in the field of organocatalysis. A variety of examples in the literature have demonstrated that cinchona alkaloids are efficient catalysts for several asymmetric reactions. Therefore, the findings of the present paper should be of practical interest when developing models for stereocontrol in cinchona alkaloid catalyzed asymmetric reactions in organic media in general.

4. Experimental Section

Synthesis of the Modifiers. *O*-Phenylcinchonidine (5). The procedure for the synthesis of *O*-phenyl derivatives of cinchona alkaloids described here is a modification of that previously published[5a] and is illustrated below for the preparation of PhOCD. Under argon atmosphere, 457 mg of NaH (19 mmol, 761 mg of 60% dispersion in mineral oil washed with absolute hexane three

times) was suspended in 30 mL of absolute DMSO and cooled with an ice-bath, whereupon cinchonidine (4 g, 13.6 mmol) was added in small portions. The reaction mixture was stirred for 1 h at 0 °C and for additional 2 h at 50 °C. To the cooled orange solution were added absolute pyridine (2.2 mL, 27.2 mmol) and CuI (2.59 g, 13.6 mmol), and the reaction mixture was stirred for 30 min. After addition of iodobenzene (1.515 mL, 13.59 mmol) the mixture was kept at 100 °C for 72 h. Water (40 mL), dichloromethane (80 mL), ethylenediaminetetraacetic acid (0.8 g), and finally concentrated ammonia solution (10 mL) were added to the reaction mixture cooled to room temperature earlier. The resulting mixture was stirred at room temperature for 1 h. The organic layer was separated, and the aqueous phase was extracted with CH_2Cl_2 (3 × 25 mL). The combined organic layers were washed with 5% ammonia solution (5 × 25 mL) until the aqueous phase remained colorless and then with water (25 mL). The solvent was removed by rotary evaporation. The residue was dissolved in EtOAc (80 mL), and the resulting solution was extracted with 2 M HCl solution (80 mL). The acidic solution was washed with EtOAc (2 × 35 mL), neutralized with solid $NaHCO_3$ until pH = 9, and extracted with EtOAc (3 × 40 mL). The combined organic layers were washed with brine, dried over Na_2SO_4, and evaporated. The product was purified over silica (120 g) using diethyl ether/triethylamine 9:1 as eluent. The solvent evaporation yielded white crystals which after recrystallization from hexane gave 2.1 g of a pure product. Yield: 42%; mp 125−127 °C. ^{1}H NMR (500 MHz, $CDCl_3$, 273.1K): δ 8.85 (d, ^3J = 4.5 Hz, 1H, H-2′), 8.21 (dd, ^4J = 1.3, ^3J = 8.5 Hz, 1H, H-8′), 8.19 (dd, ^4J = 1.3, ^3J = 8.4 Hz, 1H, H-5′), 7.82 (ddd, ^4J = 1.3, ^3J = 6.9, ^3J = 8.5 Hz, 1H, H-7′), 7.70 (ddd, ^4J = 1.3, ^3J = 6.9, ^3J = 8.4 Hz, 1H, H-6′), 7.49 (d, ^3J = 4.5 Hz, 1H, H-3′), 7.18 (m, 2H, *m*-C_6H_5), 6.91 (dd, ^4J = 0.9, ^3J = 7.3 Hz, 1H, *p*-C_6H_5), 6.79 (m, 2H, *o*-C_6H_5), 6.10 (br s, 1H, H-9), 5.75 (ddd, $^3J_{H3,H10}$ = 7.8, $^3J_{H11E,H10}$ = 10.3, $^3J_{H11Z,H10}$ = 17.1 Hz, 1H, H-10), 4.99 (ddd, ^4J = 1.2, $^3J_{H11Z,H10}$ = 17.1, ^2J = − 1.7 Hz, 1H, H-11-Z), 4.93 (ddd, ^4J = 1.0, $^3J_{H11E,H10}$ = 10.3, ^2J = − 1.7 Hz, 1H, H-11-E), 3.42 (m, 1H, H-6b), 3.25 (m, 1H, H-8), 3.20 (dd, ^3J = 10.1, ^2J = − 13.8 Hz, 1H, H-2a), 2.75 (m, 1H, H-6a), 2.72 (m, 1H, H-2b), 2.34 (m, 1H, H-3), 2.08 (m, 1H, H-7b), 1.96 (m, 1H, H-5b), 1.90 (m, 1H, H-4), 1.62 (m, 1H, H-5a), 1.56 (m, 1H, H-7a) ppm. ^{13}C NMR (150 MHz, $CDCl_3$, 298.1K): δ 157.0 (*ipso*-C_6H_5), 150.3 (C-2′), 148.5 (C-8a′), 146.5 (C-4′), 141.7 (C-10), 130.8 (C-8′), 129.6 (2C, *m*-C_6H_5), 129.3 (C-7′), 127.1 (C-6′), 125.4 (C-4a′), 122.7 (C-5′), 121.4 (*p*-C_6H_5), 118.2 (C-3′), 115.5 (2C, *o*-C_6H_5), 114.4 (C-11), 78.9 (C-9), 60.7 (C-8), 57.3 (C-2), 43.4 (C-6), 40.0 (C-3), 28.1 (C-5), 27.7 (C-4), 21.2 (C-7) ppm. $[\alpha]^{30}_D$ = +106.5° (*c* 0.048, $CHCl_3$). Analytical data for $C_{25}H_{26}N_2O$, HRMS (calcd/found): 370.2045/370.2045.

***O*-(Trimethylsilyl)cinchonine (12).** Trimethylsilyl chloride (2.16 mL, 16.81 mmol) was added dropwise to an ice-cooled solution of cinchonine (4.5 g, 15.28 mmol) in DMF (1 L) containing triethylamine (2.4 mL, 16.81 mmol) within 15 min. The reaction mixture was stirred at room temperature for 48 h until the starting material disappeared (TLC, $CHCl_3$/MeOH/triethylamine 40:10:1). The solvent was removed by rotary evaporation. The resulting oil was dissolved in 100 mL of chloroform and washed with water (100, 50, 50 mL). The water layer was extracted with additional chloroform (2 × 50 mL). Combined organic layers were washed with brine and dried over Na_2SO_4. After solvent evaporation, a white amorphous solid was obtained that recrystallized from hexane to yield 4.8 g (86%) of the product as colorless crystals. Mp = 168−173 °C (dec). ^{1}H NMR ($CDCl_3$, δ): 8.91 (d, ^3J = 4.4 Hz, 1H, H-2′), 8.63 (dd, 1H, ^4J = 1.4, ^3J = 7.9 Hz, 1H, H-5′), 8.13 (dd, ^4J = 1.4, ^3J = 7.9 Hz, 1H, H-8′), 7.75 (m, 2H, H-6′, H-7′), 7.54 (d, 1H, ^3J = 4.4 Hz, 1H, H-3′), 6.97 (s, 1H, H-9), 5.99 (m, 1H, H-10), 5.26 (m, 2H, H-11), 3.96 (m, 1H, H-2a), 3.43 (m, 2H, H-2b, H-6a), 3.28 (m, 1H, H-8), 3.20 (m, 1H, H-6b), 2.65 (m, 1H, H-3), 2.50 (m, 1H, H-7b), 2.40 (m, 1H, H-4), 1.93 (m, 1H, H-5b), 1.69 (m, 1H, H-5a), 1.15 (m, 1H, H-7a), 0.19 (s, 9H, Si-CH_3). ^{13}C NMR ($CDCl_3$, δ): 149.6 (C-2′), 148.3 (C-8a′), 145.6 (C-4′), 136.3 (C-10), 130.2 (C-8′), 129.8 (C-7′), 128.3 (C-6′), 124.5 (C-4a′), 123.1 (C-5′), 118.4 (C-3′), 117.8 (C11), 68.1 (C-9), 60.6 (C-8), 49.1 (C-6), 47.6 (C-2), 37.3 (C-3), 27.5 (C-4), 23.3 (C-5), 17.8 (C-7), 0.4 (3C, Si-CH_3). $[\alpha]^{30}_D$ = +149.9° (*c* 0.036, $CHCl_3$). Analytical data for $C_{22}H_{30}N_2OSi$, HRMS (calcd/found): 366.2127/366.2126.

Hydrogenation of 8. A 100 mg portion of **8** was dissolved in 50 mL of toluene and stirred over the Pt/Al_2O_3 catalyst (100 mg) under hydrogen pressure of 10 bar for 12−16 h. After the reaction the catalyst was filtered, the solvent was evaporated, and the sample was analyzed by NMR without further purification. *O*-(Propyldimethylsilyl)-10,11-dihydrocinchonidine (**13**): $C_{24}H_{36}N_2OSi$; ^{1}H NMR ($CDCl_3$, δ): 8.87 (d, 1H, ^3J = 4.0 Hz, H-2′), 8.20−8.10 (br, 1H, H-5′), 8.14 (d, 1H, ^3J = 8.4 Hz, H-8′), 7.72 (tr, 1H, *J* = 7.7 Hz, 1H, H-7), 7.79 (tr, 1H, *J* = 7.5 Hz, 1H, H-6′), 7.54−7.48 (br, 1H, H-3′), 5.94−5.70 (br, 1H, H-9), 3.49 (br, 1H, H-6b), 3.10 (br, 1H, H-2a), 2.98 (br, 1H, H-8), 2.70 (br, 1H, H-6a), 2.39 (br, 1H, H-2b), 1.80 (m, 1H, H-4), 1.77−1.70 (br, 1H, H-7b), 1.50−1.40 (br, 3H, H-3, H-5b, H-5a), 1.35−1.29 (m, 2H, H-13), 1.28−1.24 (br, 1H, H-7a), 1.24−1.15 (br, 2H, H-10), 0.90 (tr, ^3J = 7.2 Hz, 3H, H-14), 0.79 (tr, ^3J = 7.3 Hz, 3H, H-11), 0.55 (m, 2H, H-12) 0.07 (s, 3H, Si-CH_3-a), −0.07 (s, 3H, Si-CH_3-b). ^{13}C NMR ($CDCl_3$, δ): 149.9 (C-2′), 149.3 (br, C-8a′), 148.3 (br, C-4′), 130.4 (C-8′), 129.0 (C-7′), 126.8 (br, C-6′), 125.4 (br, C-4a′), 122.9 (br, C-5′), 118.5 (br, C-3′), 72.4 (br, C-9), 61.2 (C-8), 58.7 (C-2), 43.2 (br, C-6), 37.3 (C-3), 28.2 (br, 2C, C-5, C-7), 27.6 (C-10), 25.5 (C-4), 19.4 (C-12), 18.1 (C-14), 16.7 (C-13), 12.0 (C-11), −1.3 (Si-CH_3-b), −1.6 (Si-CH_3-a).

Additional experimental details can be found in Supporting Information.

Acknowledgment. Financial support by the Magnus Ehrnrooth Foundation (I.B.) is gratefully acknowledged. Dr. Mattias Roslund is acknowledged for fruitful discussions on the NMR results. Dr. Angelo Vargas is acknowledged for providing the information on the structures of optimized conformations for *O*-phenylcinchonidine. Computer resources provided by CSC, the Finnish IT center for science, are kindly acknowledged.

Supporting Information Available: Experimental details, atom numbering in cinchonidine derivatives, proton−proton distances, equilibrium population and torsion angles for selected cinchona alkaloids, expansion of the recorded and simulated ^{1}H NMR spectrum of TBDMSOCD (**7**), conformations of TBDMSOCD (**7**), and ^{1}H and ^{13}C NMR spectra for the synthesized compounds. This material is available free of charge via the Internet at http://pubs.acs.org.

JO8008462